

From UV to NIR: A full spectrum metal-free photocatalyst for efficient polymer synthesis in aqueous conditions

Stephanie Allison-Logan,^a Qiang Fu,^{*,a,b} Yongkang Sun,^a Min Liu,^a Jijia Xie,^c Junwang Tang,^{*,c} and Greg G Qiao^{*,a}

[a] S. Allison-Logan, Dr Q. Fu, Y. Sun, M. Liu, Prof G.G. Qiao
Polymer Science Group, Department of Chemical Engineering
University of Melbourne
Parkville, VIC 3010, Australia
E-mail: greggh@unimelb.edu.au

[b] Dr Q. Fu
Centre for Technology in Water and Wastewater (CTWW), School of Civil and Environmental Engineering
University of Technology Sydney
Ultimo, NSW 2007, Australia
E-mail: qiang.fu@uts.edu.au

[c] Dr J. Xie, Prof J. Tang
Solar Energy & Advanced Materials Research Group, Department of Chemical Engineering
University College London
Torrington Place, London WC1E 7JE, United Kingdom
E-mail: junwang.tang@ucl.ac.uk

Supporting information for this article is given via a link at the end of the document.

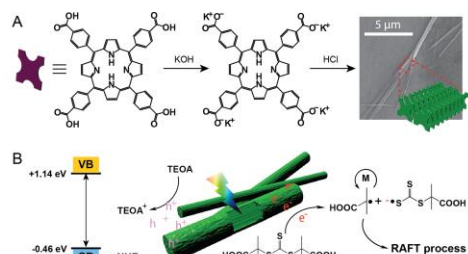
Abstract: Photo-mediation offers unparalleled spatiotemporal control over controlled radical polymerizations (CRP). Photo-induced electron/energy transfer reversible addition-fragmentation chain transfer (PET-RAFT) polymerization is particularly versatile due to its oxygen tolerance and wide range of compatible photocatalysts. In recent years, broadband- and near-infrared (NIR)-mediated polymerizations have been of particular interest due to their potential for solar-driven chemistry and biomedical applications. In this work, we present the first example of a novel photocatalyst for both full-broadband- and NIR-mediated CRP in aqueous conditions. Well-defined polymers were synthesized in water under blue, green, red, and NIR light irradiation. Exploiting the oxygen tolerant and aqueous nature of our system, we also report PET-RAFT polymerization at the microliter scale in a mammalian cell culture medium.

Photo-mediation enables spatiotemporal control of controlled/living radical polymerizations (CRP) while maintaining excellent dispersity and chain-end fidelity.^[1] For this reason, visible light-mediated reversible addition-fragmentation chain transfer (RAFT) polymerization has been studied extensively since its discovery in 2014.^[2] Such RAFT polymerization encompasses two distinct mechanisms known as photoiniferter and photo-induced electron/energy transfer (PET)-RAFT approaches. Photoiniferter RAFT polymerization requires direct activation of the RAFT agent via light irradiation and is therefore limited to wavelengths absorbed by the RAFT agent, generally UV, blue, or green light.^[3] The PET-RAFT mechanism depends on the excitation of a photoredox catalyst or a photosensitizer by light irradiation. The excited catalyst/photosensitizer interacts with the RAFT agent via energy or electron transfer to generate the initiating radical for polymerization.^[2-4] Numerous compounds have been employed as photoredox catalysts or photosensitizers for PET-RAFT polymerization including organic dyes,^[5] metalloporphyrins such as zinc tetraphenylporphyrin (ZnTPP),^[6] naturally-occurring photosynthetic pigments,^[7] enabling PET-RAFT polymerization across the visible light spectrum. Interestingly,

a photoenzymatic RAFT mechanism using flavin-dependent enzymes was recently reported, with visible light causing photoexcitation of FADH⁺ to facilitate the PET process and mediate polymerization.^[8] In addition, PET-RAFT polymerization is typically less sensitive to oxygen and can therefore be performed under less stringent conditions.^[8-9]

As PET-RAFT polymerization has gained popularity due to its versatility and less stringent reaction conditions, there has been a push to develop photocatalysts with broadband and near-infrared (NIR) absorption, due to potential “green” chemistry and biomedical applications. The solar spectrum covers wavelengths from 250-2500 nm, with IR energy alone making up nearly 50% of solar energy, while photons from visible light and NIR constitute 95% of the solar flux at sea level.^[10] Therefore, broadband and NIR absorbance are necessary to achieve efficient solar energy utilisation. In addition, NIR can penetrate opaque materials including human tissues, and therefore has potential use in biomedical applications and even *in vivo* polymerization.^[11] Boyer and coworkers reported the first NIR-mediated CRP, using bacteriochlorophyll a as a photocatalyst.^[12] More recently, they reported the use of aluminum naphthalocyanine as a photosensitizer for peroxides to initiate RAFT polymerization under NIR irradiation.^[13] The authors demonstrated temporal control and achieved high conversions even with paper, chicken skin, and pig skin barriers. These reports are significant developments in NIR-mediated photopolymerization and potential *in vivo* polymerization but to date have been limited to organic solvent.

Focusing on broadband photopolymerization, Matyjaszewski and coworkers exploited the localized surface plasmon resonance (LSPR) effect of nanostructured silver orthophosphate (Ag₃PO₄) photocatalysts.^[14] PET-RAFT polymerization of methyl acrylate demonstrated high conversions following blue, green, and red light irradiation in as well as when exposed to natural sunlight. In addition, polymerization of benzyl acrylate was possible using NIR irradiation. However, polymerization was again only limited to organic solvent.



Scheme 1. (A) The synthetic strategy for rod-like SA-TCPP and (B) schematic mechanism of the photocatalytic PET-RAFT polymerizations by SA-TCPP.

To date, all NIR-mediated CRP polymerization systems reported have been employed in organic solvents.^[12-15] However, the development of aqueous systems is essential for any potential *in vivo* applications and could also offer less expensive and more environmentally friendly options for industrial use. To aid with the development of aqueous broadband- and NIR-responsive systems, we looked to recent advances in the field of photocatalysis for solar-driven hydrogen evolution. Our group has previously reported efficient PET-RAFT polymerization with organic semiconductor graphitic carbon nitride (g-C₃N₄),^[16] an organic photocatalyst previously used in hydrogen evolution.^[17] With the use of g-C₃N₄, RAFT polymerization can be carried out with no degassing or monomer purification.^[16] Due to the limited absorbance spectrum and relatively hydrophobic surface functional groups of g-C₃N₄, its activity for polymerizations was only studied under UV irradiation in DMSO. More recently, novel photocatalysts such as covalent triazine-based framework-1 (CTF-1)^[18] and formic acid-treated carbon nitride (FAT)^[19] have shown narrower band gaps and red-shifted absorbance spectra in comparison to g-C₃N₄. Due to the improved function of these new catalysts, our previous successful PET-RAFT polymerizations using g-C₃N₄, and the need of aqueous PET-RAFT systems under NIR, we decided to investigate the use of these photocatalysts for PET-RAFT polymerization under various wavelengths in an aqueous system.

In addition, we synthesized a novel self-assembled carboxylated porphyrin (SA-TCPP) photocatalyst. Although it has been previously shown that nanometric SA-TCPP particles had a high solar spectrum efficiency and enhanced hydrogen and oxygen evolution from water under visible light irradiation,^[20] our prepared micro-size SA-TCPP photocatalyst displayed a broader absorbance spectrum from 300 to 950 nm (Figure 1A). Due to the micro-fibre like morphology, the lifetime of photoexcited electron-hole pairs is further extended, which in turn can lead to an improved polymerization efficiency compared to other recently reported photocatalysts for hydrogen evolution. As our PET-RAFT polymerization with this catalyst is in aqueous conditions under broad wavelengths, we further tested its polymerization ability in biological cell culture media, investigating its potential for *in situ* biomedical applications as well as highly efficient “green” controlled polymerizations.

We prepared the SA-TCPP photocatalyst through a modified approach. Commercially available 5,10,15,20-tetra (4-carboxy-

phenol) porphyrin (TCPP) was deprotonated in an aqueous 1M KOH solution and heated to 80 °C, yielding a purple solution. 0.1M HCl was added dropwise until the pH became neutral, following which the precipitate was purified via dialysis and freeze-dried. The resultant self-assembled TCPP (SA-TCPP) showed a dark green colour and formed long fibres/rods as seen using SEM (Scheme 1 and Figure S2). The obtained rods displayed a non-crystalline X-ray diffraction pattern and this result was further confirmed by TEM diffraction measurement (Figure 1B). Two obvious peaks at 7° and 22° represent the 1.26 nm width of an aggregated TCPP molecule and the 0.4 nm face-to-face distance between TCPP molecules. X-ray photoelectron spectroscopy (XPS) peaks assigned to carbon 1s, nitrogen 1s, and oxygen 1s were located at 285, 400, and 533 eV, respectively, and were consistent with the molecular structure of SA-TCPP (Figures 1C and S4). Furthermore, the electrochemical experiment further revealed that the prepared SA-TCPP rods exhibit a band gap of -0.46 to +1.14 eV (Figure S5).

The broad absorption spectrum of SA-TCPP allowed us to investigate its efficiency in comparison to previously reported H₂ evolution photocatalysts g-C₃N₄, CTF-1, and FAT, in water ([photocatalyst] = 2.5 mg mL⁻¹) under blue, green, and red light irradiation (Figure S7). In all cases, polymerizations performed with SA-TCPP resulted in the highest conversion. All polymerizations showed linear semi-logarithmic plots and dispersities of 1.1 or below. While all polymerizations achieved high conversions under blue light irradiation, SA-TCPP increasingly outperformed the other catalysts as the irradiation wavelength increased and was the only catalyst that led to polymer formation under red light irradiation (Figure 1D).

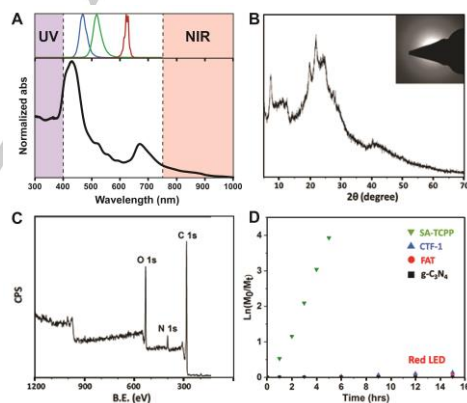


Figure 1. (A) UV-vis normalized absorption spectrum of SA-TCPP (bottom) and LED light source emission spectra (top). (B) XRD and electron diffraction patterns of SA-TCPP. (C) Full XPS spectrum of SA-TCPP. (D) Polymerization kinetics of DMA using SA-TCPP and previously reported photocatalysts under red light irradiation.

The polymerization kinetics of DMA using SA-TCPP under blue, green, red, white, and NIR irradiation are shown in Figure 2A. The use of CTF-1, FAT, and g-C₃N₄ was not investigated under NIR irradiation due to their limited absorbance spectra and poor performance under red light. In a typical reaction,

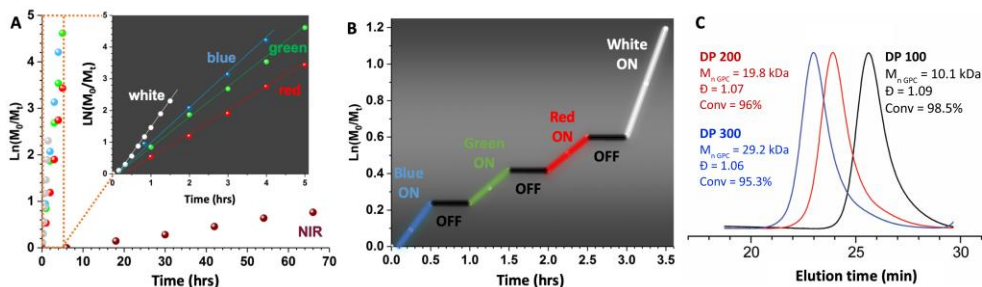


Figure 2. Kinetics of SA-TCPP-catalyzed RAFT polymerizations of DMA under (A) various LED irradiation (white to NIR, 4 mW/cm²) and (B) in an "ON/OFF" experiment. (C) GPC evolution of a *pseudo*-pentablock PDMA by chain extension. $M_{n, NMR}$ calculated from NMR for the final extended DP300 sample is 29.2 kDa as shown in Figure S9.

DMA (100 equivalents), trithiocarbonate (TTC) RAFT agent (1 equivalent), triethanolamine (TEOA, 13.4 equivalents) and SA-TCPP (5 mg) were dissolved in DI water (50 % v/v). Reaction mixtures were bubbled with argon for 20 minutes prior to light irradiation to afford faster polymerization and reduced induction period, although degassing and addition of TEOA were not essential, as previously reported (Figure S8).^[16]

The rate of polymerization was highest using white light, followed by blue, green, red, and NIR (Figure 2A). Monomer conversions of 90% or greater were achieved in 90 min using white light, 3 h with blue or green light, and 4 h with red light. Although the NIR-mediated polymerization was significantly slower, 53% conversion was reached in 66 h. These results are consistent with the absorbance spectrum of SA-TCPP shown in Figure 1A, where absorbance was greatest at blue-shifted wavelengths, as well as the higher energy of lower wavelength photons. In all cases, linear pseudo-logarithmic plots were observed indicating a constant radical concentration.

The temporal control of the system was then demonstrated using an "on/off" experiment, where the light source was turned on and off at 30 minute intervals (Figure 2B). Several cycles were performed with a different wavelength of light used during each "on" period, highlighting the broadband absorption of the photocatalyst. No polymerization was observed during the off period, demonstrating instantaneous temporal control. After 2 hours of irradiation, 70% monomer conversion was achieved. Pleasingly, the rates of polymerization during the "on" periods were in agreement with those observed in Figure 2A, with white light showing the fastest rate of polymerization, followed by blue, green, and red.

Crucially, retention of the TTC RAFT agent and its living nature were demonstrated via two chain extension reactions with greater than 95% monomer conversion attained for each block (Figure 2C). GPC traces showed symmetrical, monomodal peaks after each chain extension. Due to the symmetrical nature of the RAFT agent employed (S,S'-Bis(α , α' -dimethyl- α' -acetic acid)trithiocarbonate), the TTC moiety remained at the centre of the polymer and the two chain extensions experiments resulted in a well-defined *pseudo*-pentablock polymer.

Successful NIR-mediated polymerization with SA-TCPP suggested PET-RAFT polymerization could be performed through barriers. NIR is known to penetrate barriers, including

mammalian tissues, and the Boyer and Matyjaszewski groups have previously reported successful NIR-mediated PET-RAFT polymerization through materials such as paper and animal skin.^[13-14] Interestingly, Boyer and coworkers observed minimal change in the apparent rate propagation coefficient when polymerizing methyl acrylate through 0.1 mm paper, 1 mm chicken skin, and 2.5 mm pig skin barriers, mediated by NIR (850 nm).^[13]

Therefore, we set out to determine if we could perform our polymerization through a barrier using NIR (850 nm) and SA-TCPP in an aqueous environment. We carried out our investigation using a piece of opaque paper wrapped around the reaction vessel as a barrier. An induction period of 6 hours was observed before achieving 30% conversion after 66 h (Figure 3B). The GPC trace of the resulting polymer was monomodal and symmetrical, with a low dispersity of 1.07, as shown in Figure 3C. To our knowledge, this is the first time NIR irradiation has been used for CRP polymerization in water. These results signify an essential step towards biocompatible NIR-mediated polymerization, where an aqueous system would be essential.

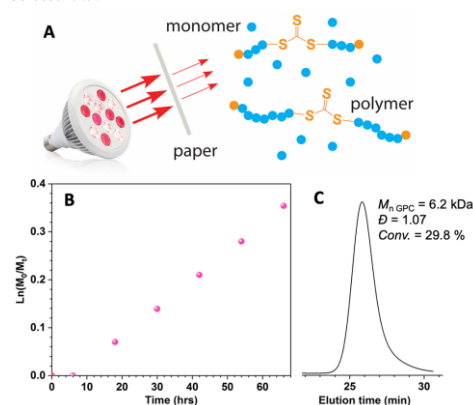


Figure 3. (A) Schematic illustration of an opaque paper barrier employed for polymerizations under NIR LED light ($\lambda_{max} = 850$ nm). (B) Kinetic study of SA-

TCPP catalyzed RAFT polymerization of DMA under NIR LED irradiation (4 mW/cm²). (C) GPC curve of the resultant PDMA.

Any *in vivo* polymerizations would also need to be biocompatible and performed with a low volume. To this end, we attempted a preliminary study of the PET-RAFT polymerization using PEG methacrylate (PEGMA, 480 Da) in the presence of mammalian fibroblast cells in a 96-well plate (Figure 4A). Six wells each contained 0.13 mg SA-TCPP, 22 mg PEGMA, 0.7 mg TTC, and 0.5 mg TEOA in complete DMEM cell culture medium to a total volume of 100 μ L. The 96-well plate was irradiated with red light for 45 minutes at 37 $^{\circ}$ C. The conversion of PEGMA was 11% and GPC characterization showed a monomodal peak with a small tail (Figure 4B). Significantly, this work demonstrates our system can conduct polymerization without degassing at microliter scale, offering the future potential for machine programmable multi-block polymerization via computer-controlled microliter injection systems. We also measured cell viability immediately following light irradiation and obtained 46% cell viability (Figure 4C). While optimization of reaction conditions and reagents is needed to reduce the toxicity of the system, these preliminary results suggest a biocompatible, NIR-mediated PET-RAFT polymerization may soon be possible.

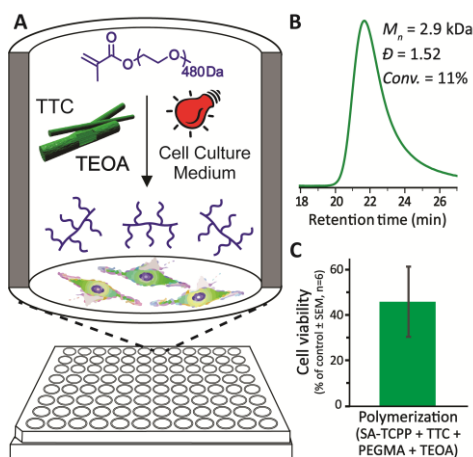


Figure 4. (A) Microliter-scale PET-RAFT polymerization of PEGMA₄₈₀ in a 96-well plate containing fibroblast cells, 45 minutes red light irradiation. (B) GPC trace of poly(PEGMA), and (C) cell viability following PET-RAFT polymerization.

The recent reports by the Boyer,^[12-13] Matyjaszewski,^[14] and Yagci^[15a] groups demonstrate exciting developments in broadband- and NIR-mediated CRP. Building on these critical advances, we report for the first time an aqueous NIR-mediated CRP. The use of a metal-free, porphyrin-based organic photocatalyst with an absorbance spectrum covering 300-950 nm enabled broadband- and NIR-mediated PET-RAFT polymerization in water. SA-TCPP was compared to three other photocatalysts previously reported for hydrogen evolution and

was found to have the highest rate of polymerization when irradiated with white, blue, green, and red light. Preliminary investigations resulted in the successful microliter-scale polymerization of PEGMA in the presence of mammalian cells in complete cell culture medium, with future works to focus on improving cell viability. These findings have broad implications for potential *in vivo* polymerizations for biomedical applications as well as “green” polymerizations.

Acknowledgements

G.G.Q. acknowledges the Australian Research Council’s Discover Project (DP170104321). S.A.-L. is the recipient of a Melbourne International Engagement Award. M.L. acknowledges support from the China Scholarship Council-University of Melbourne Research Scholarship (201606260063). Q.F. acknowledges the Australian Research Council under the Future Fellowship (FT180100312). J.X. and J.T. are thankful for the financial support from the Royal Society Newton Advanced Fellowship grant (NAFR1\191163) and Leverhulme Trust (RPG-2017-122).

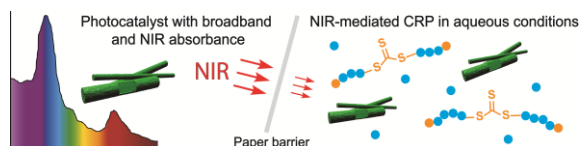
Keywords: RAFT polymerization • photocatalysis • NIR • photopolymerization

- [1] a) T. G. McKenzie, Q. Fu, M. Uchiyama, K. Satoh, J. Xu, C. Boyer, M. Kamigaito, G. G. Qiao, *Adv. Sci.* **2016**, *3*, 1500394; b) N. D. Dolinski, Z. A. Page, E. H. Discekici, D. Meis, I. H. Lee, G. R. Jones, R. Whitfield, X. Pan, B. G. McCarthy, S. Shanmugam, *J. Polym. Sci., Part A: Polym. Chem.* **2019**, *57*, 268-273.
- [2] J. Xu, K. Jung, A. Atme, S. Shanmugam, C. Boyer, *Journal of the American Chemical Society* **2014**, *136*, 5508-5519.
- [3] a) T. G. McKenzie, Q. Fu, E. H. Wong, D. E. Dunstan, G. G. Qiao, *Macromolecules* **2015**, *48*, 3864-3872; b) J. Yeow, O. R. Sugita, C. Boyer, *ACS Macro Lett.* **2016**, *5*, 558-564; c) S. b. Perrier, *Macromolecules* **2017**, *50*, 7433-7447.
- [4] N. Corrigan, J. Xu, C. Boyer, X. Allonas, *ChemPhotoChem* **2019**, *3*, 1193-1199.
- [5] a) C. A. Figg, J. D. Hickman, G. M. Scheutz, S. Shanmugam, R. N. Carmean, B. S. Tucker, C. Boyer, B. S. Sumerlin, *Macromolecules* **2018**, *51*, 1370-1376; b) S. Shanmugam, S. Xu, N. N. M. Adnan, C. Boyer, *Macromolecules* **2018**, *51*, 779-790; c) J. Xu, S. Shanmugam, H. T. Duong, C. Boyer, *Polym. Chem.* **2015**, *6*, 5615-5624; d) N. Corrigan, L. Zernakov, M. H. Hashim, J. Xu, C. Boyer, *React. Chem. Eng.* **2019**, *4*, 1216-1228.
- [6] a) A. J. Gormley, J. Yeow, G. Ng, O. Conway, C. Boyer, R. Chapman, *Angew. Chem. Int. Ed.* **2018**, *57*, 1557-1562; b) K. Satoh, Z. Sun, M. Uchiyama, M. Kamigaito, J. Xu, C. Boyer, *Polym. J.* **2019**, *1-9*; c) M. Li, M. Fromel, D. Ranaweera, S. Rocha, C. Boyer, C. Pester, *ACS Macro Lett.* **2019**, *8*, 374-380; d) P. Seal, J. Xu, S. De Luca, C. Boyer, S. C. Smith, *Adv. Theory Simul.* **2019**, *2*, 1900038.
- [7] a) S. Shanmugam, J. Xu, C. Boyer, *Chemical Science* **2015**, *6*, 1341-1349; b) J. M. Ren, T. G. McKenzie, Q. Fu, E. H. Wong, J. Xu, Z. An, S. Shanmugam, T. P. Davis, C. Boyer, G. G. Qiao, *Chemical Reviews* **2016**, *116*, 6743-6836; c) C. Wu, S. Shanmugam, J. Xu, J. Zhu, C. Boyer, *Chem. Commun.* **2017**, *53*, 12560-12563.
- [8] F. Zhou, R. Li, X. Wang, S. Du, Z. An, *Angewandte Chemie International Edition* **2019**, *58*, 9479-9484.
- [9] a) L. Zhang, C. Wu, K. Jung, Y. H. Ng, C. Boyer, *Angew. Chem. Int. Ed.* **2019**, *131*, 16967-16970; b) N. Zaquen, A. M. Kadir, A. Iasa, N. Corrigan, T. Junkers, P. B. Zetterlund, C. Boyer, *Macromolecules* **2019**, *52*, 1609-1619.

-
- [10] a) M. Q. Yang, M. Gao, M. Hong, G. W. Ho, *Adv. Mater.* **2018**, *30*, 1802894; b) L. Liang, X. Li, Y. Sun, Y. Tan, X. Jiao, H. Ju, Z. Qi, J. Zhu, Y. Xie, *Joule* **2018**, *2*, 1004-1016.
- [11] N. Corrigan, J. Yeow, P. Judzewitsch, J. Xu, C. Boyer, *Angew. Chem. Int. Ed.* **2019**, *58*, 5170-5189.
- [12] S. Shanmugam, J. Xu, C. Boyer, *Angew. Chem. Int. Ed.* **2016**, *55*, 1036-1040.
- [13] Z. Wu, K. Jung, C. Boyer, *Angew. Chem. Int. Ed.* **2020**, *59*, 2013-2017.
- [14] J. Jiang, G. Ye, F. Lorandi, Z. Liu, Y. Liu, T. Hu, J. Chen, Y. Lu, K. Matyjaszewski, *Angew. Chem. Int. Ed.* **2019**, *58*, 12096-12101.
- [15] a) C. Kütahya, C. Schmitz, V. Strehmel, Y. Yagci, B. Strehmel, *Angew. Chem. Int. Ed.* **2018**, *57*, 7898-7902; b) C. Tian, P. Wang, Y. Ni, L. Zhang, Z. Cheng, X. Zhu, *Angew. Chem. Int. Ed. Engl.* **2020**, *59*, 3910-3916.
- [16] Q. Fu, Q. Ruan, T. G. McKenzie, A. Reyhani, J. Tang, G. G. Qiao, *Macromolecules* **2017**, *50*, 7509-7516.
- [17] X. Wang, K. Maeda, A. Thomas, K. Takanabe, G. Xin, J. M. Carlsson, K. Domen, M. Antonietti, *Nat. Mater.* **2009**, *8*, 76-80.
- [18] J. Xie, S. A. Shevlin, Q. Ruan, S. J. A. Moniz, Y. Liu, X. Liu, Y. Li, C. C. Lau, Z. X. Guo, J. Tang, *Energy Environ. Sci.* **2018**, *11*, 1617-1624.
- [19] Y. Wang, F. Silveri, M. K. Bayazit, Q. Ruan, Y. Li, J. Xie, C. R. A. Catlow, J. Tang, *Adv. Energy Mater.* **2018**, *8*, 1801084.
- [20] Z. Zhang, Y. Zhu, X. Chen, H. Zhang, J. Wang, *Adv. Mater.* **2019**, *31*, e1806626.

Entry for the Table of Contents

Insert graphic for Table of Contents here.



Insert text for Table of Contents here.

Photopolymerizations mediated by broadband and near-infrared (NIR) light are of intense interest due to their potential use in solar-driven and *in vivo* applications. Employing a novel metal-free photocatalyst and PET-RAFT approach, we present the first broadband- and NIR-mediated controlled radical polymerization in aqueous media, including cell culture medium, marking a crucial advance towards *in vivo* polymerization for biomedical applications.

Formatted: English (United Kingdom)

Formatted: Normal, Space Before: 0 pt